

***SparseLLM*: Towards Global Pruning of Pre-trained Language Models**

Guangji Bai¹ Yijiang Li² Chen Ling¹ Kibaek Kim² Liang Zhao^{1,*}

¹Emory University ²Argonne National Laboratory

*Corresponding Author

{guangji.bai, chen.ling, liang.zhao}@emory.edu

{yijiang.li, kimk}@anl.gov

Abstract

The transformative impact of large language models (LLMs) like LLaMA and GPT on natural language processing is countered by their prohibitive computational demands. Pruning has emerged as a pivotal compression strategy, introducing sparsity to enhance both memory and computational efficiency. Yet, traditional global pruning is impractical for LLMs due to scalability issues, while local pruning, despite its efficiency, leads to suboptimal solutions. Addressing these challenges, we propose *SparseLLM*, a novel framework that redefines the global pruning process into manageable, coordinated subproblems, allowing for resource-efficient optimization with global optimality. *SparseLLM*'s approach, which conceptualizes LLMs as a chain of modular functions and leverages auxiliary variables for problem decomposition, not only facilitates a pragmatic application on LLMs but also demonstrates significant performance improvements, particularly in high-sparsity regimes where it surpasses current state-of-the-art methods. *Code* can be found at <https://github.com/BaiTheBest/SparseLLM>.

1 Introduction

Large language models (LLMs) Touvron et al. [2023], OpenAI [2023] have recently transformed the field of natural language processing (NLP) by delivering exceptional results across a variety of intricate language benchmarks Wei et al. [2022], Bommarito II and Katz [2022], Bubeck et al. [2023]. Nonetheless, these models, with billions of parameters, generally necessitate significant computational resources. To make LLMs more accessible, extensive efforts have been devoted to model compression of LLMs Xu and McAuley [2023], Bai et al. [2024], including pruning, quantization, knowledge distillation, and low-rank factorization. *Pruning*, by introducing *sparsity*, jointly enhances memory and computational efficiency and offers unparalleled flexibility, seamlessly integrating with any LLMs, thus standing out as a highly effective and widely adopted compression strategy.

Model pruning has a long history LeCun et al. [1989] and has proven effective in applications related to vision and smaller language models Hoefer et al. [2021]. However, conventional pruning techniques, which rely on global pruning and require loading the entire model into the same GPU Mallya and Lazebnik [2018], Singh and Alistarh [2020], become impractical for today's LLMs due to their vast size. Recently, several *local pruning* methods, which consider compressing each layer separately, and the overall compressed model is then obtained by "stitching together" the individually compressed layers, are proposed for billion-scale LLMs. SparseGPT Frantar and Alistarh [2023], an efficient unstructured pruning method for LLMs with hundreds of billions of parameters, achieves up to 60% parameter reduction with minimal performance loss. Another approach, Wanda Sun et al. [2023], introduces a novel pruning criterion that evaluates weights by considering both magnitude and related input activations. Despite its efficiency gains, local pruning only aims to minimize the local error for

each specific layer under sparsity constraints, resulting in a *suboptimal* solution for the overall model. This is because local pruning *over-aligns* the intermediate layers’ activations, leading to suboptimal performance, especially in high-sparsity regimes Singh and Alistarh [2020], Sung et al. [2023].

To address these challenges and achieve global pruning with low memory consumption, we propose *SparseLLM* that decomposes the global pruning objective into multiple subproblems, each of which can be solved with low resources and coordinate to achieve the global pruning objective. More specifically, we first formulate LLMs as a composite function where the output of one module is the input of the next. Based on this formulation, we reformulate the global pruning goal into an equivalent form with auxiliary variables that facilitate its decomposition and coordination of the subproblems. Then we propose an alternating optimization algorithm to efficiently solve the subproblems, achieving computational resource efficiency and global optimality, due to the close-form solution of each subproblem. Empirically, we find that *SparseLLM* can consistently improve the performance of local pruning methods, particularly in high sparsity regimes ($> 60\%$), where the perplexity can be significantly decreased by up to around 80% as compared to the state-of-the-art methods.

Furthermore, our *SparseLLM* framework can be readily applicable to enhance the performance of most existing local pruning solvers, such as SparseGPT and Wanda, with marginal additional computational overhead. This adaptability ensures that our framework can be seamlessly integrated into a wide range of LLMs and pruning methods, making it a versatile tool and useful baseline for future research exploiting the sparsity of LLMs.

2 Related work

Pruning, a pivotal concept in machine learning that introduces sparsity into neural networks, dates back to the 1980s LeCun et al. [1989]. It gained renewed attention in the late 2010s, especially for deep neural networks, under the banner of reducing inference costs Han et al. [2015]. LLM pruning techniques can broadly be categorized into *structured* and *unstructured* prunings.

Unstructured pruning looks at simplifying the complexity of LLMs by removing certain parameters *regardless* of the model’s inherent structure. This approach typically involves setting a threshold to nullify parameters below it, leading to a model with a non-uniform sparse structure. SparseGPT Frantar and Alistarh [2023], an efficient unstructured pruning method for LLMs with hundreds of billions of parameters, achieves up to 60% parameter reduction with minimal performance loss. A novel pruning criterion is introduced in Wanda Sun et al. [2023], which evaluates weights by considering both magnitude and related input activations. This approach is beneficial in linear layers of LLMs, helping to identify and remove less significant weights. Tuli and Jha Tuli and Jha [2023] proposed DynaTran, a dynamic inference scheme for pruning activations at runtime, supported by a specially designed ASIC architecture, AccelTran, to enhance transformer inference throughput.

On the other hand, structured pruning involves the selective removal of groups of weights, where “group” might mean blocks of weights, filters, attention heads, or other structures conducive to hardware acceleration. Ma et al. Ma et al. [2023] introduced the LLM-Pruner, a framework designed for structured pruning of LLMs, which utilizes a combination of first-order data and Hessian information for effective importance estimation. This aids in identifying crucial groups for pruning. Li et al. Li et al. [2023] proposed LoSparse, a novel approach combining low-rank and sparse matrix approximations to balance pruning and expressive power. Tao et al. Tao et al. [2023] extended this concept to pruning hidden dimensions in LLMs, including embedding layers and attention heads. ZipLM Kurtic et al. [2023], a structured compression method for LLMs, is proposed to optimize for compression and accuracy while considering specific hardware constraints.

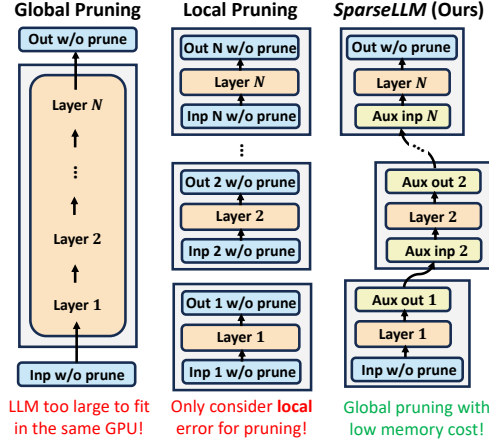


Figure 1: *SparseLLM* decomposes the global pruning of LLMs into manageable subproblems by leveraging the chain of modules and auxiliary variables while maintaining dependencies.

Our work falls in the category of unstructured pruning of LLMs, where existing methods such as SparseGPT and Wanda only consider an *entirely local* pruning algorithm and suffer from *suboptimal* performance. We discuss the limitations and challenges of entirely local pruning in Sec. 3.

3 Background and notation

3.1 Global pruning

Given a pre-trained neural network f with parameter \mathbf{W} and inputs \mathbf{X} , global pruning aims to find a global sparsity mask \mathbf{M} and possibly updated weights $\widehat{\mathbf{W}}$ to minimize the *global loss* \mathcal{L} between the final outputs of the uncompressed and compressed model:

$$\min_{\mathbf{M}, \widehat{\mathbf{W}}} \mathcal{L}(f(\mathbf{X}; \mathbf{M} \odot \widehat{\mathbf{W}}), f(\mathbf{X}; \mathbf{W})), \quad (1)$$

where \odot denotes the *element-wise* multiplication. In addition to NP-hardness Blumensath and Davies [2008], however, a critical challenge in solving Eq. 1 is the huge memory cost, as one needs to store the entire model in a single GPU, rendering this method impractical for modern billion-scale LLMs.

3.2 Local pruning

Local pruning circumvents the memory issue mentioned above by dividing the full model compression into subproblems for each layer and constructing a *local loss* to measure the ℓ_2 -error between the outputs of the uncompressed and compressed layers. Hence, the local pruning can be formulated by

$$\min_{\mathbf{M}_\ell, \widehat{\mathbf{W}}_\ell} \|\mathbf{W}_\ell \cdot \mathbf{X}_\ell - (\mathbf{M}_\ell \odot \widehat{\mathbf{W}}_\ell) \cdot \mathbf{X}_\ell\|_2^2. \quad (2)$$

Although smaller than the global pruning, the local pruning still needs to optimize both the mask \mathbf{M}_ℓ and the remaining weights $\widehat{\mathbf{W}}_\ell$ and thus remains NP-hard. Therefore, exactly solving it for larger layers is unrealistic, leading all existing methods to resort to approximations.

Mask selection & weight reconstruction. A particularly popular approach is to separate the problem into *mask selection* and *weight reconstruction* Hubara et al. [2021], Kwon et al. [2022]. Concretely, this means first choosing a pruning mask \mathbf{M} according to some salient criterion, like the weight magnitude Zhu and Gupta [2017], and then optimizing the remaining unpruned weights while keeping the mask unchanged. Importantly, once the mask is fixed, Eq. 2 turns into a *linear regression* problem that can be easily optimized.

Existing solvers. Early work Kingdon and Kingdon [1997] applied iterated linear regression to small networks. Recently, the AdaPrune approach Hubara et al. [2021] has shown good results for this problem on modern models via magnitude-based weight selection, followed by applying SGD steps to reconstruct the remaining weights. Follow-up works demonstrate that pruning accuracy can be further improved by removing the strict separation between mask selection and weight reconstruction. More recently, Frantar and Alistarh [2023] developed SparseGPT, an efficient unstructured pruning method for LLMs with hundreds of billions of parameters, achieving up to 60% parameter reduction with minimal performance loss. Sun et al. [2023] introduced a novel pruning criterion in Wanda, which evaluates weights by considering both magnitude and related input activations.

3.3 What is wrong with local pruning?

As shown in Eq. 2, local pruning focuses on minimizing the error for each specific layer ℓ subject to sparsity constraints. This results in a suboptimal solution with respect to the global pruning problem. While the primary goal of pruning is to ensure that the input and output of the pruned model align closely with those of the original models, the local pruning overly constrains the activations of all the intermediate layers between the two models, leading to performance degradation.

4 SparseLLM: Towards global pruning for LLMs

We present our proposed method SparseLLM that can address the drawbacks of existing pruning methods by achieving a global pruning with low memory consumption. SparseLLM decomposes the global pruning objective into many subproblems, each of which can be solved using low resources and can coordinate each other toward the global pruning objective. An overview of SparseLLM on the OPT and LLaMA configurations are shown in Figure 2.

4.1 Motivation

The development of SparseLLM is motivated by the observation: LLMs can be formulated as a composite function such that the output of one module is the input of the next. This allows us to reformulate the global pruning goal into its equivalent form with auxiliary variables that enable the decomposition into multiple subproblems, as detailed in Sec. 4.2. Then we develop a resource-efficient algorithm that achieves the alternating optimization of the subproblems with global optimality, thanks to the close-form solution of each subproblem, as illustrated in Sec. 4.3.

4.2 A unified formulation of pruning

In this section, we present the reformulation of the global pruning problem into an equivalent one by introducing auxiliary variables. This reformulation provides a more flexible form and enables the decomposition of the problem into many manageable subproblems.

The key idea behind our formulation is to decouple the densely parametric parts (linear layers) from non-parametric parts (activation function, self-attention, layer norm, etc) using a splitting technique. Rather than feeding the output of the dense linear layer \mathbf{W}_ℓ directly into the non-parametric and potentially nonlinear layer ϕ_ℓ , we store the output of layer ℓ in a new variable $\mathbf{z}_\ell = \mathbf{W}_\ell \mathbf{a}_{\ell-1}$ ¹. We also represent the output of the non-parametric layer as a vector of activations $\mathbf{a}_\ell = \phi_\ell(\mathbf{z}_\ell)$. We then solve the following problem:

$$\begin{aligned} & \min_{\{\widehat{\mathbf{W}}_\ell\}, \{\mathbf{M}_\ell\}, \{\mathbf{a}_\ell\}, \{\mathbf{z}_\ell\}} \mathcal{L}(\mathbf{z}_L, \mathbf{y}), \\ \text{s.t. } & \mathbf{z}_\ell = (\mathbf{M}_\ell \odot \widehat{\mathbf{W}}_\ell) \mathbf{a}_{\ell-1}, \forall \ell \in [L], \\ & \mathbf{a}_\ell = \phi_\ell(\mathbf{z}_\ell), \forall \ell \in \Omega, \\ & \mathbf{a}_\ell, \mathbf{z}_\ell = \mathbf{a}_\ell^{pre}, \mathbf{z}_\ell^{pre}, \forall \ell \in [L-1] \setminus \Omega, \end{aligned} \quad (3)$$

where L represents the total number of dense (linear) layers and $[L] = \{1, 2, \dots, L\}$. $[L-1] \setminus \Omega$ denotes the complement set of Ω . We use $\mathbf{a}_\ell^{pre}, \mathbf{z}_\ell^{pre}$ to denote the corresponding intermediate variables' values of the original dense (i.e., *without* pruning) pre-trained model. \mathbf{y} denotes the ground-truth final output of the dense pre-trained model.

In our proposed formulation above, its unified nature lies in the interpretation and application of the set Ω , which denotes the indices of layers subject to the pruning process. Intuitively, Ω measures how ‘‘global’’ the pruning is. The bigger the set of Ω is, the more layers are connected via the second constraint, and the pruning is more towards the global extreme, and vice versa. The generality and versatility of our formulation is illustrated in the following remark:

Remark 4.1 (Generality and flexibility of Eq. 3). *Given an LLM formulated as a composite function with dense layers $\ell \in \{1, 2, \dots, L-1\}$, where L is the total number of dense layers and Ω denotes the set of layers subject to the pruning process. Our formulation can seamlessly treat both global and local pruning as special cases under certain conditions. Specifically:*

- When $\Omega = \{1, 2, \dots, L-1\}$, solving our pruning formulation is equivalent to global pruning, accounting for inter-layer dependencies across the entire network.
- When $\Omega = \emptyset$, the formulation simplifies to local pruning, considering each layer independently (the last constraint dominates and ‘‘cuts’’ all layer dependencies with pre-trained values.)

The ability to shift between these two extremes, and potentially any intermediate configurations, demonstrates the flexibility and comprehensiveness of our formulation. By adjusting Ω , one can seamlessly transition from a global perspective to a local perspective. This flexibility not only caters to a wide range of pruning strategies but also provides a unified framework to compare and contrast the effectiveness of different pruning methods under a consistent mathematical lens.

4.3 Algorithm design

In this section, we introduce the algorithm design of *SparseLLM*, which alternatively optimizes the subproblems associated with the corresponding variables. This approach is resource-efficient and achieves global optimality, attributed to the closed-form solutions that each subproblem yields.

¹For the sake of simplicity and clearer presentation, the bias term is omitted in the following equations where its exclusion does not lead to confusion.

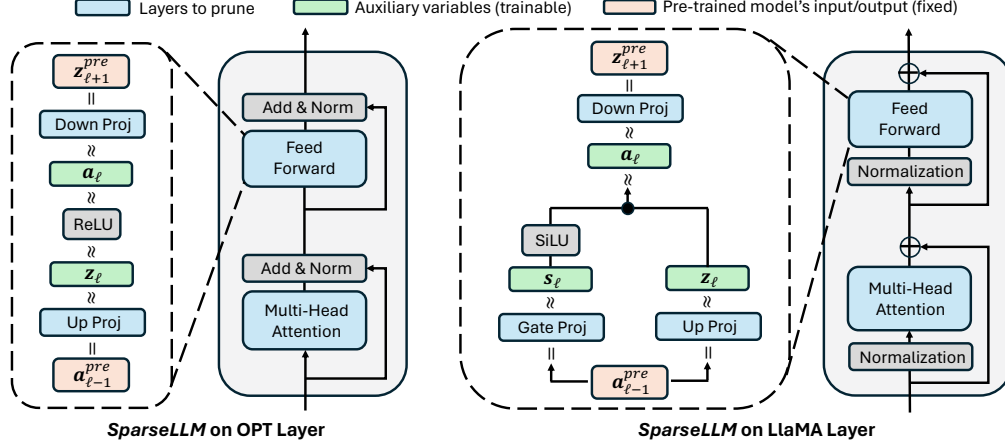


Figure 2: Illustration of *SparseLLM* on OPT and LLaMA. The auxiliary variables and soft constraints (i.e., \approx) allow *SparseLLM* to decompose the global pruning into manageable subproblems while maintaining the dependencies. Subproblems are *analytically* solvable and enjoy fast convergence.

The key idea of our algorithm lies behind the flexibility of Ω in our Eq. 3, as we want to find a better trade-off between completely global (memory bottleneck) and completely local (suboptimal performance) pruning. Naively applying *SparseLLM* to prune all layers globally is impractical. On the other hand, recent work shows that the feed-forward network (FFN) module in each decoder layer accounts for more than *two-thirds* of the total parameters in an LLM Liu et al. [2024]. Therefore, our *SparseLLM* prioritizes the global pruning of the FFN module, while still adhering to a local pruning strategy for the multi-head attention (MHA) module (see Figure 2). This strategy strikes a balance between the computational feasibility of pruning large-scale models and the effectiveness of the pruning process, adhering to the limitations and practices of state-of-the-art LLM pruning frameworks.

Formally speaking, rather than try to solve Eq. 3 directly, we first relax the constraints by adding an ℓ_2 -penalty function to the objective and attack the unconstrained problem:

$$\mathcal{L}(\mathbf{z}_L, \mathbf{y}) + \alpha \sum_{\ell \in [L]} \|\mathbf{z}_\ell - (\mathbf{M}_\ell \odot \widehat{\mathbf{W}}_\ell) \mathbf{a}_{\ell-1}\|_2^2 + \beta \sum_{\ell \in \Omega_{\text{FFN}}} \|\mathbf{a}_\ell - \phi_\ell(\mathbf{z}_\ell)\|_2^2, \quad (4)$$

where α, β are hyperparameters for controlling the weight of each constraint. Ω_{FFN} denotes the set of indexes for the linear layers in the FFN module of each decoder layer, i.e., linear layers from the same FFN module are pruned globally. For simplicity, the superscript “pre” of \mathbf{a}_ℓ and \mathbf{z}_ℓ in the third constraint in Eq. 3 is omitted here, i.e., for $\ell \notin \Omega_{\text{FFN}}$ the \mathbf{a}_ℓ and \mathbf{z}_ℓ are fixed and equal to the pre-trained model’s intermediate value in the second term of Eq. 4. In the following subsections, we illustrate how we approach the pruning of FFN and MHA modules, respectively.

4.3.1 *SparseLLM* on OPT models

For each decoder layer in a pre-trained LLM, our Eq. 4 instantly simplifies to globally pruning the corresponding FFN module within that decoder layer as:

$$\alpha \|\mathbf{z}_{\ell+1}^{pre} - (\mathbf{M}_{\ell+1} \odot \widehat{\mathbf{W}}_{\ell+1}) \mathbf{a}_\ell\|_2^2 + \beta \|\mathbf{a}_\ell - \phi_\ell(\mathbf{z}_\ell)\|_2^2 + \alpha \|\mathbf{z}_\ell - (\mathbf{M}_\ell \odot \widehat{\mathbf{W}}_\ell) \mathbf{a}_{\ell-1}^{pre}\|_2^2, \quad (5)$$

where layers ℓ and $\ell + 1$ correspond to the up-projection and down-projection linear layers.

In this work, we consider the *alternating* method to optimize our Eq. 5, i.e., optimize each variable while keeping the rest fixed. The careful and elaborate design of our Eq. 5 allows us to derive a *closed-form* solution to every subproblem as shown in the following.

Pruning weight. First consider optimizing Eq. 5 with respect to \mathbf{M}_ℓ and $\widehat{\mathbf{W}}_\ell$. For each linear layer ℓ in a FFN module, the optimal solution minimizes $\|\mathbf{z}_\ell - (\mathbf{M}_\ell \odot \widehat{\mathbf{W}}_\ell) \mathbf{a}_{\ell-1}\|_2^2$. To solve it, the first step is to decompose \mathbf{z}_ℓ to $\mathbf{W}_\ell \mathbf{a}_{\ell-1}$, where $\mathbf{W}_\ell = \mathbf{z}_\ell \mathbf{a}_{\ell-1}^\dagger$ (\dagger denotes the pseudo-inverse.) Plug decomposed \mathbf{z}_ℓ back in original loss and we get $\|\mathbf{W}_\ell \mathbf{a}_{\ell-1} - (\mathbf{M}_\ell \odot \widehat{\mathbf{W}}_\ell) \mathbf{a}_{\ell-1}\|_2^2$, which aligns with the pruning objective of Eq. 2 and can be analytically solved by existing pruning solver e.g., SparseGPT. The superscript of “pre” for $\mathbf{a}_{\ell-1}$ is omitted in this section for simpler notation.

Updating activation. Minimization for \mathbf{a}_ℓ is a simple least-squares problem similar to weight pruning. However, in this case, the matrix $\mathbf{a}_{\ell-1}$ appears in two penalty terms in Eq. 5, so we must minimize $\alpha \|\mathbf{z}_{\ell+1}^{pre} - (\mathbf{M}_{\ell+1} \odot \widehat{\mathbf{W}}_{\ell+1})\mathbf{a}_\ell\|_2^2 + \beta \|\mathbf{a}_\ell - \phi_\ell(\mathbf{z}_\ell)\|_2^2$ for \mathbf{a}_ℓ , holding all other variables fixed. By following a very similar idea to Ridge regression, the new value of \mathbf{a}_ℓ is given by:

$$(\alpha \mathbf{W}_{\ell+1}^\top \mathbf{W}_{\ell+1} + \beta \mathbf{I})^{-1} (\alpha \mathbf{W}_{\ell+1}^\top \mathbf{z}_{\ell+1}^{pre} + \beta \cdot \text{ReLU}(\mathbf{z}_\ell)), \quad (6)$$

where \mathbf{W}_ℓ denotes the updated weight matrix after pruning, i.e., $\mathbf{W}_\ell := \mathbf{M}_\ell \odot \widehat{\mathbf{W}}_\ell$.

Updating output. The update for \mathbf{z}_ℓ requires minimizing the following loss:

$$\beta \|\mathbf{a}_\ell - \text{ReLU}(\mathbf{z}_\ell)\|_2^2 + \alpha \|\mathbf{z}_\ell - (\mathbf{M}_\ell \odot \widehat{\mathbf{W}}_\ell) \mathbf{a}_{\ell-1}^{pre}\|_2^2. \quad (7)$$

This problem is non-convex and non-quadratic (because of the non-linear function ReLU). Fortunately, because the ReLU function works entry-wise on its argument, the entries in \mathbf{z}_ℓ are de-coupled. Solving Eq. 7 is particularly easy for the case of ReLU, as it can be solved in closed form followed by a simple if-then logic. Specifically, one only needs to compute two solutions of a quadratic equation:

$$\mathbf{z}_\ell^{(1)} = (\mathbf{M}_\ell \odot \widehat{\mathbf{W}}_\ell) \mathbf{a}_{\ell-1}^{pre}, \quad \mathbf{z}_\ell^{(2)} = (\alpha + \beta)^{-1} \cdot (\beta \mathbf{a}_\ell + \alpha \mathbf{z}_\ell^{(1)}), \quad (8)$$

where the first solution corresponds to those entries of \mathbf{z}_ℓ that are negative (reduced to zero by ReLU), and the second solution corresponds to those entries of \mathbf{z}_ℓ that are non-negative.

4.3.2 SparseLLM on LLaMA models

In this section, we introduce how *SparseLLM* decomposes global pruning into subproblems and solves them iteratively on LLaMA model families. The model architecture of LLaMA can be found in Figure 2. Overall, *SparseLLM* operates similarly on both LLaMA and OPT models, with the main difference being that LLaMA includes an additional dense linear layer, known as the gate projection layer, and uses the SiLU activation function instead of ReLU.

Pruning weight. In this part, *SparseLLM* functions almost identically to its operation on OPTs.

Updating activation \mathbf{a}_ℓ . Similarly, for updating \mathbf{a}_ℓ , *SparseLLM* works nearly the same as on OPT. The minimization for \mathbf{a}_ℓ is a simple least-squares problem, akin to weight pruning. However, in this case, the matrix $\mathbf{a}_{\ell-1}$ appears in two penalty terms in Eq. 5, necessitating the minimization of:

$$\alpha \|\mathbf{z}_{\ell+1}^{pre} - (\mathbf{M}_{\ell+1} \odot \widehat{\mathbf{W}}_{\ell+1})\mathbf{a}_\ell\|_2^2 + \beta \|\mathbf{a}_\ell - \text{SiLU}(\mathbf{s}_\ell) \odot \mathbf{z}_\ell\|_2^2, \quad (9)$$

for \mathbf{a}_ℓ , with all other variables held fixed. Following a concept similar to Ridge regression, the updated value of \mathbf{a}_ℓ is:

$$(\alpha \mathbf{W}_{\ell+1}^\top \mathbf{W}_{\ell+1} + \beta \mathbf{I})^{-1} (\alpha \mathbf{W}_{\ell+1}^\top \mathbf{z}_{\ell+1}^{pre} + \beta \cdot \text{SiLU}(\mathbf{s}_\ell) \odot \mathbf{z}_\ell), \quad (10)$$

where \mathbf{W}_ℓ denotes the updated weight matrix after pruning, i.e., $\mathbf{W}_\ell := \mathbf{M}_\ell \odot \widehat{\mathbf{W}}_\ell$.

Updating output \mathbf{z}_ℓ . Updating \mathbf{z}_ℓ is somewhat simpler in LLaMA since the activation function applies over the gate projection layer. The update requires minimizing the loss:

$$\beta \|\mathbf{a}_\ell - \text{SiLU}(\mathbf{s}_\ell) \odot \mathbf{z}_\ell\|_2^2 + \alpha \|\mathbf{z}_\ell - (\mathbf{M}_\ell \odot \widehat{\mathbf{W}}_\ell) \mathbf{a}_{\ell-1}^{pre}\|_2^2. \quad (11)$$

This problem is quadratic when solving for \mathbf{z}_ℓ with other variables fixed. Through mathematical manipulations, the analytical solution for \mathbf{z}_ℓ is found by solving a quadratic equation:

$$\mathbf{z}_\ell^* = \frac{(\mathbf{M}_\ell \odot \widehat{\mathbf{W}}_\ell) \mathbf{a}_{\ell-1}^{pre} + \text{SiLU}(\mathbf{s}_\ell) \odot \mathbf{a}_\ell}{\text{SiLU}(\mathbf{s}_\ell)^2 + \mathbf{1}}, \quad (12)$$

where the division is element-wise and $\mathbf{1}$ denotes the all-one matrix.

Updating gate projection output \mathbf{s}_ℓ . Updating \mathbf{s}_ℓ involves minimizing:

$$\beta \|\mathbf{a}_\ell - \text{SiLU}(\mathbf{s}_\ell) \odot \mathbf{z}_\ell\|_2^2 + \alpha \|\mathbf{s}_\ell - (\mathbf{M}_s \odot \widehat{\mathbf{W}}_s) \mathbf{a}_{\ell-1}^{pre}\|_2^2, \quad (13)$$

where \mathbf{M}_s and $\widehat{\mathbf{W}}_s$ denote the mask and layer weights for the gate projection layer. This problem is non-convex and non-quadratic due to the non-linear SiLU function. However, since SiLU operates entry-wise, the entries in \mathbf{s}_ℓ are decoupled. Despite LLaMA lacking a simple closed-form solution as in OPT (which uses ReLU), the problem can still be solved quickly and analytically using a lookup table of pre-computed solutions, since each element in \mathbf{s}_ℓ depends on only three variables.

Remark 4.2 (Global convergence of SparseLLM). *Consider the objective function given by Eq. 5, under the condition that the activation function ϕ is ReLU. Notice that (1) the objective function is convex with respect to each variable when all others are fixed, and (2) given that closed-form solutions exist for the subproblems in the alternating optimization scheme, the proposed algorithm is guaranteed to converge to a global optimum.*

4.3.3 Pruning of MHAs

SparseLLM also prunes other linear layers besides those in FFNs. By following Eq. 4, for each linear layer out of FFN modules, the pruning objective simplifies to $\alpha \|\mathbf{z}_{\ell+1}^{pre} - (\mathbf{M}_{\ell+1} \odot \widehat{\mathbf{W}}_{\ell+1}) \mathbf{a}_{\ell}^{pre}\|_2^2$, which is equivalent (with some simple math) to that of completely local pruning as shown in Eq. 2. Existing LLM pruning solvers such as SparseGPT and Wanda are applicable here.

4.4 Time complexity analyses

The proposed *SparseLLM* consists of three main steps, with the overall time complexity being the sum of the complexities of these steps. In the weights pruning step, the complexity is dominated by the pseudo-inverse computation of matrix \mathbf{a}_{ℓ} (dimensions $n \times h$), which is $O(nh^2)$. Using SparseGPT as the solver, the exact pruning step has a complexity of $O(h^3)$. The second step, updating activation, involves matrix inversion of the weight matrix \mathbf{W}_{ℓ} (size $h \times h$) with a complexity of $O(h^3)$. The third step, updating outputs, has a lower complexity. Thus, the overall algorithm complexity is bounded by $O(h^3)$, making our method’s per-epoch time complexity comparable to SparseGPT.

5 Experiments

Experiments setup. We implement *SparseLLM* in PyTorch Paszke et al. [2019] and use the HuggingFace Transformers library Wolf et al. [2019] for handling models and datasets. All pruning experiments are conducted on NVIDIA A100 GPUs. For calibration data, we follow Frantar and Alistarh [2023] and use 128 2048-token segments, randomly chosen from the first shard of the C4 Raffel et al. [2020] dataset. This represents generic text data crawled from the internet and ensures our experiments remain zero-shot as no task-specific data is seen during pruning. *We followed existing work Frantar and Alistarh [2023], Sun et al. [2023] and pruned all linear layers (in FFN and MHA) to the target sparsity.*

Models, datasets & evaluation. We consider the OPT model family Zhang et al. [2022] and LLaMA-2 model family Touvron et al. [2023] in our experiments. We show results on different sizes of models to provide a broader picture for the performances of *SparseLLM*. In terms of metrics, we mainly focus on perplexity, which is known to be a challenging and stable metric that is well-suited for evaluating the accuracy of compression methods Yao et al. [2022], Dettmers and Zettlemoyer [2023]. We consider the test sets of raw-WikiText2 Merity et al. [2016] (WT2) and PTB Marcus et al. [1994] as well as a subset of the C4 validation data, all popular benchmarks in LLM compression literature Yao et al. [2022], Park et al. [2022], Frantar and Alistarh [2023], Sun et al. [2023]. For additional interpretability, we also provide zero-shot accuracy results following the same setup of Sun et al. [2023], which is based on the popular EleutherAI-eval harness Gao et al. [2023].

Comparison methods. We compare against three baselines, magnitude pruning Zhu and Gupta [2017] applied locally, and two other state-of-the-art local pruning methods, SparseGPT Frantar and Alistarh [2023] and Wanda Sun et al. [2023].

5.1 Results and analyses

Pruning vs. model sizes. We begin by exploring the pruning capabilities of *SparseLLM* across various model sizes in comparison to baseline methods. For each model, we consider unstructured sparsity ranging from 70% to 90% with a 10% increment, as well as a 3:4 semi-structured sparsity. The 3:4 semi-structured sparsity is inspired by our preliminary results that suggest good performance *SparseLLM* at high sparsity regimes. However, note that two of our baselines, Magnitude and Wanda, are unable to be configured to this sparsity out-of-box. We conduct a sensitivity study on the calibration sample sizes (see Appendix A.3) and use calibration sample sizes between 32 and 64 for all experiments. Moreover, we prune the first 50% of the Transformer decoder layers in each model to achieve a balance between the computation resources and the performances. Detailed results can be found in Table 1 and Table 5 (see Appendix A.5). The perplexity results of the dense models are reported next to the names of the models.

Table 1: Perplexity in high sparsity regimes ($\geq 70\%$); the lower the perplexity, the better.

OPT-1.3b (WikiText2 (WT2): 14.62; PTB: 20.29; C4: 16.07)												
Sparsity	70%			80%			90%			3:4		
Dataset	WT2	PTB	C4	WT2	PTB	C4	WT2	PTB	C4	WT2	PTB	C4
Magnitude	6420.80	4828.13	3435.99	9998.71	1.1e4	5347.89	8209.13	1.0e4	4917.02	-	-	-
Wanda	21.56	34.77	25.78	142.20	146.76	142.24	5692.65	4751.69	4501.73	-	-	-
SparseGPT	18.04	28.19	21.45	69.67	93.36	60.83	2596.70	2361.86	1363.08	252.81	238.41	146.21
SparseLLM	17.82	27.72	20.99	58.92	85.33	58.36	1350.31	1192.36	655.76	128.83	144.48	106.01
OPT-2.7b (WikiText2 (WT2): 12.47; PTB: 17.97; C4: 14.32)												
Sparsity	70%			80%			90%			3:4		
Dataset	WT2	PTB	C4	WT2	PTB	C4	WT2	PTB	C4	WT2	PTB	C4
Magnitude	1691.74	1237.08	1415.02	1.0e4	7916.69	6050.07	7.9e5	5.3e5	4.7e5	-	-	-
Wanda	88.61	140.09	90.06	6140.81	4746.96	5678.66	3.0e4	3.5e4	2.4e4	-	-	-
SparseGPT	13.79	21.18	16.18	24.32	37.82	25.92	2662.74	2285.01	1776.08	91.02	91.79	64.95
SparseLLM	13.82	21.07	16.14	23.87	37.09	24.90	1200.12	759.11	527.70	56.90	77.14	52.77
OPT-30b (WikiText2 (WT2): 9.56; PTB: 14.04; C4: 11.45)												
Sparsity	70%			80%			90%			3:4		
Dataset	WT2	PTB	C4	WT2	PTB	C4	WT2	PTB	C4	WT2	PTB	C4
Magnitude	8691.40	4769.89	4732.66	8941.81	5292.98	5092.26	3.8e7	3.0e7	1.4e7	-	-	-
Wanda	7766.61	5547.45	5741.74	8770.33	6020.70	7132.20	6354.15	4296.37	4654.27	-	-	-
SparseGPT	9.58	14.41	11.93	16.49	22.01	17.67	5747.87	5169.50	3555.24	441.35	464.73	209.44
SparseLLM	9.56	14.40	11.94	15.61	19.64	16.61	3050.63	2712.39	1758.63	51.28	73.61	37.99
OPT-66b (WikiText2 (WT2): 9.34; PTB: 13.36; C4: 10.99)												
Sparsity	70%			80%			90%			3:4		
Dataset	WT2	PTB	C4	WT2	PTB	C4	WT2	PTB	C4	WT2	PTB	C4
Magnitude	OOM	OOM	OOM	OOM	OOM	OOM	OOM	OOM	OOM	-	-	-
Wanda	OOM	OOM	OOM	OOM	OOM	OOM	OOM	OOM	OOM	-	-	-
SparseGPT	9.45	13.64	11.37	28.27	57.41	26.26	7803.10	6594.88	4433.35	6594.37	6329.59	3799.87
SparseLLM	9.37	13.66	11.37	16.45	21.00	17.70	7504.17	5644.65	3683.91	4641.8	5296.93	1618.43
LlaMA-2 7b (WikiText2 (WT2): 5.47; PTB: 37.91; C4: 7.26)												
Sparsity	70%			80%			90%			3:4		
Dataset	WT2	PTB	C4	WT2	PTB	C4	WT2	PTB	C4	WT2	PTB	C4
Magnitude	1058.00	544.43	889.46	6380.27	NaN	4162.92	9498.91	1.02e4	7539.65	-	-	-
Wanda	2644.22	4040.95	1630.09	1814.01	3376.35	1124.26	5206.93	4607.30	2780.45	-	-	-
SparseGPT	15.98	302.15	18.58	53.20	803.02	52.57	344.97	2503.82	279.77	68.28	784.79	60.45
SparseLLM	16.15	274.35	18.23	49.96	664.39	47.39	225.23	2233.52	181.56	64.17	667.27	54.56
LlaMA-2 13b (WikiText2 (WT2): 4.88; PTB: 50.94; C4: 6.73)												
Sparsity	70%			80%			90%			3:4		
Dataset	WT2	PTB	C4	WT2	PTB	C4	WT2	PTB	C4	WT2	PTB	C4
Magnitude	30.34	2317.39	28.48	4133.98	4706.65	4112.69	5580.71	5514.22	5090.63	-	-	-
Wanda	23.42	502.53	32.65	295.29	2340.13	261.15	3003.49	3804.69	1738.73	-	-	-
SparseGPT	12.98	267.63	15.95	45.59	550.59	45.20	825.99	1410.46	673.33	63.48	660.70	56.29
SparseLLM	12.95	277.76	15.77	36.36	578.35	38.63	646.15	1078.94	466.98	53.71	632.11	50.40

From the table, it shows a general trend of increasing perplexity with increasing sparsity. Moreover, we observe a trend of decreasing perplexity for SparseGPT and *SparseLLM* at the same sparsity with increasing model sizes. However, such a trend is not obvious for Magnitude and Wanda. We also observe that SparseGPT and *SparseLLM* consistently outperform Magnitude and Wanda by a significant margin. For smaller sparsity, *SparseLLM* achieves comparable perplexity to SparseGPT. As we increase the sparsity, *SparseLLM* starts to demonstrate noticeable improvements over SparseGPT. In numerous instances for the OPT model family, *SparseLLM* achieves perplexity reductions of more than

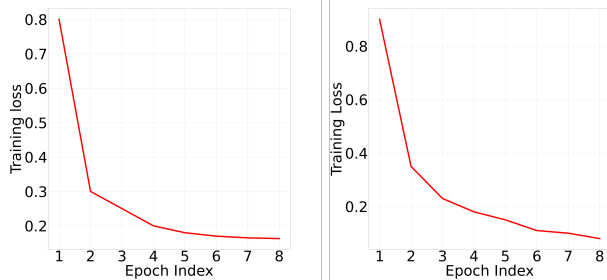


Figure 3: **Fast convergence** of *SparseLLM*. Training loss per epoch for pruning layer 3 of OPT-125m at 80% sparsity (**Left**) and layer 6 of LlaMA-2 13b at 70% sparsity (**Right**).

Table 2: Accuracy (%) of zero-shot tasks; the higher the accuracy, the better.

OPT-30b								
Sparsity	Method	BoolQ	RTE	HellaSwag	WinoGrandeARC-e	ARC-c	OBQA	Mean
Dense		70.46	61.82	54.27	69.02	70.47	35.49	55.96
70%	SparseGPT	68.78	58.48	53.83	67.64	69.15	34.30	54.54
	SparseLLM	69.11	61.73	53.97	68.43	69.78	34.73	55.36
80%	SparseGPT	64.86	60.65	49.73	61.40	61.91	31.74	50.64
	SparseLLM	65.41	59.57	50.65	61.96	62.71	32.25	51.29
90%	SparseGPT	37.83	53.79	25.96	49.88	26.47	12.60	32.39
	SparseLLM	43.55	52.35	26.32	50.04	27.31	20.56	33.45
3:4	SparseGPT	55.81	51.26	33.64	54.54	42.05	21.33	39.95
	SparseLLM	60.83	54.15	39.35	55.41	45.24	24.06	43.03
LlaMA-2 7b								
Sparsity	Method	BoolQ	RTE	HellaSwag	WinoGrandeARC-e	ARC-c	OBQA	Mean
Dense		75.05	66.43	56.92	69.93	75.34	41.89	59.99
70%	SparseGPT	68.26	57.04	39.67	59.04	60.9	28.58	47.73
	SparseLLM	67.61	57.31	40.12	61.39	59.39	28.76	48.13
80%	SparseGPT	59.36	52.71	28.83	48.7	34.22	18.34	36.65
	SparseLLM	60.12	53.07	28.62	50.59	34.55	18.69	37.13
90%	SparseGPT	39.02	52.34	26.66	47.80	28.32	17.37	31.99
	SparseLLM	39.45	52.71	26.79	51.17	28.32	19.52	32.92
3:4	SparseGPT	53.94	54.15	28.09	49.17	31.57	17.41	35.59
	SparseLLM	57.34	53.43	28.26	48.86	32.45	18.17	36.13
LlaMA-2 13b								
Sparsity	Method	BoolQ	RTE	HellaSwag	WinoGrandeARC-e	ARC-c	OBQA	Mean
Dense		77.89	70.40	59.94	72.77	77.40	46.50	62.59
70%	SparseGPT	70.03	53.43	42.20	66.54	64.94	25.40	50.60
	SparseLLM	69.87	54.15	42.50	68.64	64.97	31.40	51.05
80%	SparseGPT	62.69	52.71	28.94	50.91	36.24	18.17	37.67
	SparseLLM	64.39	52.86	29.19	51.46	35.69	18.77	38.08
90%	SparseGPT	50.21	51.35	26.71	49.14	26.68	13.2	33.86
	SparseLLM	55.35	52.05	26.89	51.34	27.35	19.62	35.26
3:4	SparseGPT	61.28	53.71	28.40	47.99	33.21	18.26	36.69
	SparseLLM	61.71	55.71	28.56	51.62	32.11	18.49	37.43

50% compared to SparseGPT. We also see that performance improvements from *SparseLLM* over SparseGPT are more significant for the OPT model family than the LlaMA-2 model family.

Zero-shot experiments. To further conclude the evaluations and discussions, we show results for several zero-shot tasks in Table 2 and Table 6 (see Appendix A.5) comparing SparseGPT and *SparseLLM*. These evaluations are known to be relatively noisy Dettmers et al. [2022], but more interpretable. We also report the results for zero-shot tasks from the dense models in the “Dense” row. We see that the accuracy of both methods decreases with increasing sparsity, which is expected, as more parameters are pruned. A similar trend of increasing accuracy with increasing model size is observed too. Across all the tasks, OBQA and ARC-c remain the most challenging ones as the accuracy for both methods is 30% or below 30% while both methods perform well for BoolQ, RTE, WinoGrande, and ARC-e. In general, *SparseLLM* is able to achieve higher accuracy in the majority of tasks across the models of different sizes in both OPT and LlaMA-2 model families.

Training loss vs. epochs in *SparseLLM*. Figure 3 illustrates the change in training loss over epochs for *SparseLLM*, with the training loss plotted on a scale of 10^3 for clarity. We observe that the training loss decreases rapidly during the initial epochs, highlighting the efficiency of *SparseLLM* in achieving effective global pruning within a short period. This rapid convergence is largely due to the closed-form solutions employed by *SparseLLM* for various subproblems, which streamline the pruning process and ensure optimal layer-wise pruning without extensive iterative computations. These analytical solutions enable *SparseLLM* to perform precise pruning operations quickly, making it a powerful tool for optimizing large-scale models like LlaMA, significantly reducing model size while maintaining high accuracy.

6 Conclusion

Our work presents *SparseLLM*, a cutting-edge framework poised to redefine the compression of LLMs through sparsity. By adeptly circumventing the scalability issues of global pruning and optimizing the local suboptimality of existing methods, *SparseLLM* stands as a significant advancement in the field. Our empirical results affirm its efficacy, particularly in high-sparsity environments, where it achieves a notable reduction in perplexity, thereby setting a new precedent for model compression. The versatility and minimal computational overhead of *SparseLLM* complement its integration with current pruning technologies, underscoring its potential as a universal tool for enhancing the performance and accessibility of LLMs.

References

- G. Bai, Z. Chai, C. Ling, S. Wang, J. Lu, N. Zhang, T. Shi, Z. Yu, M. Zhu, Y. Zhang, et al. Beyond efficiency: A systematic survey of resource-efficient large language models. *arXiv preprint arXiv:2401.00625*, 2024.
- T. Blumensath and M. E. Davies. Iterative thresholding for sparse approximations. *Journal of Fourier analysis and Applications*, 14:629–654, 2008.
- M. Bommarito II and D. M. Katz. Gpt takes the bar exam. *arXiv preprint arXiv:2212.14402*, 2022.
- S. Bubeck, V. Chandrasekaran, R. Eldan, J. Gehrke, E. Horvitz, E. Kamar, P. Lee, Y. T. Lee, Y. Li, S. Lundberg, et al. Sparks of artificial general intelligence: Early experiments with gpt-4. *arXiv preprint arXiv:2303.12712*, 2023.
- T. Dettmers and L. Zettlemoyer. The case for 4-bit precision: k-bit inference scaling laws. In *International Conference on Machine Learning*, pages 7750–7774. PMLR, 2023.
- T. Dettmers, M. Lewis, Y. Belkada, and L. Zettlemoyer. Llm.int8(): 8-bit matrix multiplication for transformers at scale. *arXiv preprint arXiv:2208.07339*, 2022.
- E. Frantar and D. Alistarh. Massive language models can be accurately pruned in one-shot. *arXiv preprint arXiv:2301.00774*, 2023.
- L. Gao, J. Tow, B. Abbasi, S. Biderman, S. Black, A. DiPofi, C. Foster, L. Golding, J. Hsu, A. Le Noac’h, H. Li, K. McDonell, N. Muennighoff, C. Ociepa, J. Phang, L. Reynolds, H. Schoelkopf, A. Skowron, L. Sutawika, E. Tang, A. Thite, B. Wang, K. Wang, and A. Zou. A framework for few-shot language model evaluation, 12 2023. URL <https://zenodo.org/records/10256836>.
- S. Han, H. Mao, and W. J. Dally. Deep compression: Compressing deep neural networks with pruning, trained quantization and huffman coding. *arXiv preprint arXiv:1510.00149*, 2015.
- T. Hoefer, D. Alistarh, T. Ben-Nun, N. Dryden, and A. Peste. Sparsity in deep learning: Pruning and growth for efficient inference and training in neural networks. *The Journal of Machine Learning Research*, 22(1):10882–11005, 2021.
- I. Hubara, B. Chmiel, M. Island, R. Banner, J. Naor, and D. Soudry. Accelerated sparse neural training: A provable and efficient method to find $n:m$ transposable masks. *Advances in neural information processing systems*, 34:21099–21111, 2021.
- J. Kingdon and J. Kingdon. Hypothesising neural nets. *Intelligent Systems and Financial Forecasting*, pages 81–106, 1997.
- E. Kurtic, E. Frantar, and D. Alistarh. Ziplm: Hardware-aware structured pruning of language models. *arXiv preprint arXiv:2302.04089*, 2023.
- W. Kwon, S. Kim, M. W. Mahoney, J. Hassoun, K. Keutzer, and A. Gholami. A fast post-training pruning framework for transformers. *Advances in Neural Information Processing Systems*, 35: 24101–24116, 2022.
- Y. LeCun, J. Denker, and S. Solla. Optimal brain damage. *Advances in neural information processing systems*, 2, 1989.

- Y. Li, Y. Yu, Q. Zhang, C. Liang, P. He, W. Chen, and T. Zhao. Lospase: Structured compression of large language models based on low-rank and sparse approximation. *arXiv preprint arXiv:2306.11222*, 2023.
- Z. Liu, Q. Song, Q. C. Xiao, S. K. Selvaraj, R. Mazumder, A. Gupta, and X. Hu. Ffsplit: Split feed-forward network for optimizing accuracy-efficiency trade-off in language model inference. *arXiv preprint arXiv:2401.04044*, 2024.
- X. Ma, G. Fang, and X. Wang. Llm-pruner: On the structural pruning of large language models. *arXiv preprint arXiv:2305.11627*, 2023.
- A. Mallya and S. Lazebnik. Packnet: Adding multiple tasks to a single network by iterative pruning. In *Proceedings of the IEEE conference on Computer Vision and Pattern Recognition*, pages 7765–7773, 2018.
- M. Marcus, G. Kim, M. A. Marcinkiewicz, R. MacIntyre, A. Bies, M. Ferguson, K. Katz, and B. Schasberger. The penn treebank: Annotating predicate argument structure. In *Human Language Technology: Proceedings of a Workshop held at Plainsboro, New Jersey, March 8-11, 1994*, 1994.
- S. Merity, C. Xiong, J. Bradbury, and R. Socher. Pointer sentinel mixture models. *arXiv preprint arXiv:1609.07843*, 2016.
- R. OpenAI. Gpt-4 technical report. arxiv 2303.08774. *View in Article*, 2:13, 2023.
- G. Park, B. Park, S. J. Kwon, B. Kim, Y. Lee, and D. Lee. nuqmm: Quantized matmul for efficient inference of large-scale generative language models. *arXiv preprint arXiv:2206.09557*, 2022.
- A. Paszke, S. Gross, F. Massa, A. Lerer, J. Bradbury, G. Chanan, T. Killeen, Z. Lin, N. Gimelshein, L. Antiga, et al. Pytorch: An imperative style, high-performance deep learning library. *Advances in neural information processing systems*, 32, 2019.
- C. Raffel, N. Shazeer, A. Roberts, K. Lee, S. Narang, M. Matena, Y. Zhou, W. Li, and P. J. Liu. Exploring the limits of transfer learning with a unified text-to-text transformer. *The Journal of Machine Learning Research*, 21(1):5485–5551, 2020.
- S. P. Singh and D. Alistarh. Woodfisher: Efficient second-order approximation for neural network compression. *Advances in Neural Information Processing Systems*, 33:18098–18109, 2020.
- M. Sun, Z. Liu, A. Bair, and J. Z. Kolter. A simple and effective pruning approach for large language models. *arXiv preprint arXiv:2306.11695*, 2023.
- Y.-L. Sung, J. Yoon, and M. Bansal. Ecoflap: Efficient coarse-to-fine layer-wise pruning for vision-language models. *arXiv preprint arXiv:2310.02998*, 2023.
- C. Tao, L. Hou, H. Bai, J. Wei, X. Jiang, Q. Liu, P. Luo, and N. Wong. Structured pruning for efficient generative pre-trained language models. In *Findings of the Association for Computational Linguistics: ACL 2023*, pages 10880–10895, 2023.
- H. Touvron, L. Martin, K. Stone, P. Albert, A. Almahairi, Y. Babaei, N. Bashlykov, S. Batra, P. Bhargava, S. Bhosale, et al. Llama 2: Open foundation and fine-tuned chat models. *arXiv preprint arXiv:2307.09288*, 2023.
- S. Tuli and N. K. Jha. Acceltran: A sparsity-aware accelerator for dynamic inference with transformers. *IEEE Transactions on Computer-Aided Design of Integrated Circuits and Systems*, 2023.
- J. Wei, Y. Tay, R. Bommasani, C. Raffel, B. Zoph, S. Borgeaud, D. Yogatama, M. Bosma, D. Zhou, D. Metzler, et al. Emergent abilities of large language models. *arXiv preprint arXiv:2206.07682*, 2022.
- T. Wolf, L. Debut, V. Sanh, J. Chaumond, C. Delangue, A. Moi, P. Cistac, T. Rault, R. Louf, M. Funtowicz, et al. Huggingface’s transformers: State-of-the-art natural language processing. *arXiv preprint arXiv:1910.03771*, 2019.

- C. Xu and J. McAuley. A survey on model compression and acceleration for pretrained language models. In *Proceedings of the AAAI Conference on Artificial Intelligence*, volume 37, pages 10566–10575, 2023.
- Z. Yao, R. Yazdani Aminabadi, M. Zhang, X. Wu, C. Li, and Y. He. Zeroquant: Efficient and affordable post-training quantization for large-scale transformers. *Advances in Neural Information Processing Systems*, 35:27168–27183, 2022.
- S. Zhang, S. Roller, N. Goyal, M. Artetxe, M. Chen, S. Chen, C. Dewan, M. Diab, X. Li, X. V. Lin, et al. Opt: Open pre-trained transformer language models. *arXiv preprint arXiv:2205.01068*, 2022.
- M. Zhu and S. Gupta. To prune, or not to prune: exploring the efficacy of pruning for model compression. *arXiv preprint arXiv:1710.01878*, 2017.

A Appendix

This section includes supplemental materials (pseudo-code, additional experiments, and plots).

A.1 Pseudo-code of *SparseLLM*

Algorithm 1 *SparseLLM* Pruning of OPT Models.

Input: An OPT decoder layer containing FFN and MHA modules. FFN’s up-scaling linear layer pre-trained weight matrix \mathbf{W}_ℓ , FFN’s down-scaling linear layer pre-trained weight matrix $\mathbf{W}_{\ell+1}$, input of the up-scaling linear layer $\mathbf{a}_{\ell-1}^{pre}$, output of the down-scaling linear layer $\mathbf{z}_{\ell+1}^{pre}$, target sparsity ρ , constraint weight hyperparameters α, β .

```

1 SparseLLM on FFN():
2   Initialize  $\mathbf{z}_\ell = \mathbf{z}_\ell^{pre}$ ,  $\mathbf{a}_\ell = \mathbf{a}_\ell^{pre}$  ▷ Initialize slack variables
   Pre-compute and cache  $\mathbf{a}_{\ell-1}^\dagger = \text{pseudo-inverse}(\mathbf{a}_{\ell-1}^{pre})$ 
   for step  $i = 1, \dots, K$  do
3      $\mathbf{W}_\ell = \mathbf{z}_\ell \mathbf{a}_{\ell-1}^\dagger$ ,  $\mathbf{W}_{\ell+1} = \mathbf{z}_{\ell+1} \mathbf{a}_\ell^\dagger$ 
      $\mathbf{M}_\ell, \widehat{\mathbf{W}}_\ell = \arg \min \|\mathbf{W}_\ell \mathbf{a}_{\ell-1}^{pre} - (\mathbf{M}_\ell \odot \widehat{\mathbf{W}}_\ell) \mathbf{a}_{\ell-1}^{pre}\|_2^2$  ▷ Prune layer  $\ell$  by SparseGPT solver
      $\mathbf{M}_{\ell+1}, \widehat{\mathbf{W}}_{\ell+1} = \arg \min \|\mathbf{W}_{\ell+1} \mathbf{a}_\ell - (\mathbf{M}_{\ell+1} \odot \widehat{\mathbf{W}}_{\ell+1}) \mathbf{a}_\ell\|_2^2$  ▷ Prune layer  $\ell + 1$  by SparseGPT solver
      $\mathbf{W}_{\ell+1} = \mathbf{M}_{\ell+1} \odot \widehat{\mathbf{W}}_{\ell+1}$ ,  $\mathbf{W}_\ell = \mathbf{M}_\ell \odot \widehat{\mathbf{W}}_\ell$ 
      $\mathbf{a}_\ell = (\alpha \mathbf{W}_{\ell+1}^\top \mathbf{W}_{\ell+1} + \beta \mathbf{I})^{-1} (\alpha \mathbf{W}_{\ell+1}^\top \mathbf{z}_{\ell+1}^{pre} + \beta \phi_\ell(\mathbf{z}_\ell))$  ▷ Update activations
      $\mathbf{z}_\ell^{(1)} = \mathbf{W}_\ell \mathbf{a}_{\ell-1}^{pre}$ ,  $\mathbf{z}_\ell^{(2)} = (\alpha + \beta)^{-1} \cdot (\beta \mathbf{a}_\ell + \alpha \mathbf{z}_\ell^{(1)})$ ,
     for  $j = 1, \dots, n$  in parallel do
4       if  $(\mathbf{z}_\ell)_j < 0$  then
5          $(\mathbf{z}_\ell)_j = (\mathbf{z}_\ell^{(1)})_j$  ▷ Update outputs
6       else
7          $(\mathbf{z}_\ell)_j = (\mathbf{z}_\ell^{(2)})_j$  ▷ Update outputs
8   return  $\mathbf{W}_\ell, \mathbf{W}_{\ell+1}$ 
9 SparseLLM on MHA():
10  for each linear layer  $\ell$  in MHA module do
11    Fix  $\mathbf{z}_\ell = \mathbf{z}_\ell^{pre}$ ,  $\mathbf{a}_\ell = \mathbf{a}_\ell^{pre}$  ▷ Fix intermediate variables
     $\mathbf{M}_\ell, \widehat{\mathbf{W}}_\ell = \arg \min \|\mathbf{W}_\ell \mathbf{a}_{\ell-1}^{pre} - (\mathbf{M}_\ell \odot \widehat{\mathbf{W}}_\ell) \mathbf{a}_{\ell-1}^{pre}\|_2^2$  ▷ Prune layer  $\ell$  by SparseGPT solver
12  return  $\{\mathbf{W}_\ell\}$  for all linear layers in MHA

```

The *SparseLLM* algorithm presented in Algorithm 1 demonstrates how *SparseLLM* works on an OPT decoder layer. The key inputs to the algorithm include the pre-trained weight matrices for both the up-scaling and down-scaling linear layers of the FFN, along with a set of hyperparameters and a sparsity constraint. The goal of *SparseLLM* is to achieve a targeted level of sparsity in the linear layers without significantly compromising the model’s performance.

Initiating with the pre-trained weights, *SparseLLM* employs a series of pruning and activation update steps across K iterations. In each iteration, it solves optimization problems to prune the current and subsequent layer weights, followed by updating the activation variables. The utilization of SparseGPT solvers for pruning and the strategic update of activations ensures that the pruned network approximates the original network’s behavior as closely as possible. The final output of the algorithm is a pair of pruned weight matrices for the consecutive layers, which are expected to deliver comparable or improved performance with a reduced number of parameters.

A.2 Two-layer Demo on the Details behind our Global Pruning

Figure 4 illustrates the *SparseLLM* pruning method compared to conventional global pruning and local pruning, using a two-layer neural network as an abstraction for simplicity. The figure is divided into three main parts:

On the left, conventional global pruning is depicted. This method applies a global mask to the entire network, resulting in significant memory costs due to poor scalability. Both functions f_1 and f_2 are pruned using the same mask across all layers, leading to high memory usage.

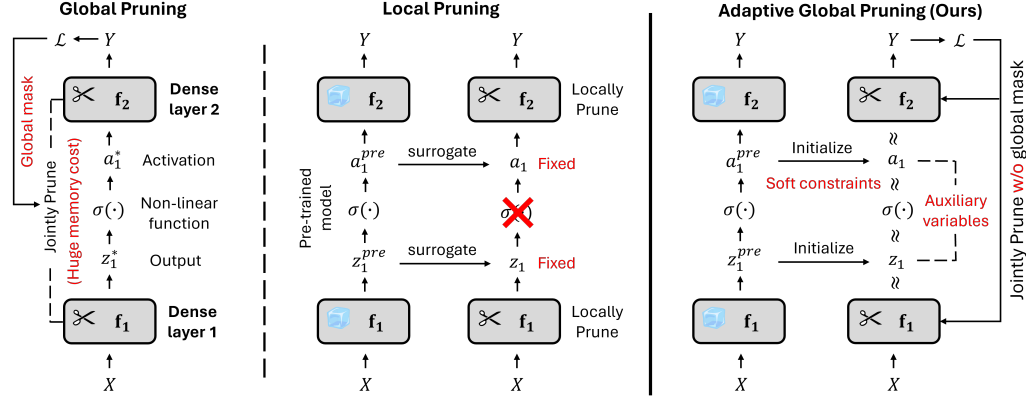


Figure 4: **Illustration of *SparseLLM* pruning method** compared to *conventional global pruning* and *local pruning*. We consider a *two-layer* neural network as an abstraction for simplicity. *Global pruning* (left) is memory prohibitive due to poor scalability. *Local pruning* (mid) considers pruning each layer independently, while inevitably sacrificing performance due to the ignorance of global supervision. Our adaptive global pruning (right) achieves global pruning with low memory cost by leveraging auxiliary variables and soft constraints.

In the middle, local pruning is shown, where each layer is pruned independently. This approach reduces memory costs by applying separate masks to each layer. However, it inevitably sacrifices performance because it ignores global supervision, which can lead to suboptimal pruning decisions that do not consider the network as a whole.

On the right, the adaptive global pruning method of *SparseLLM* is presented. This method achieves global pruning with low memory cost by leveraging auxiliary variables and soft constraints. It combines the benefits of global pruning—considering the entire network structure—with efficient memory usage. The introduction of auxiliary variables allows for flexible and adaptive pruning, ensuring that the overall performance of the network is maintained while keeping memory costs low.

Thus, the figure highlights the trade-offs between different pruning strategies. Conventional global pruning incurs high memory costs, local pruning reduces memory usage at the expense of performance, and the adaptive global pruning of *SparseLLM* strikes a balance by maintaining performance with lower memory requirements through the use of auxiliary variables and soft constraints.

A.3 Calibration Samples

Figure 5 and Figure 6 present how perplexity changes with the calibration sample sizes on the datasets PTB and C4 for OPT-2.7b and LLaMA-2 7B, respectively. In both figures, as the number of calibration samples increases, the perplexity decreases for both *SparseGPT* and *SparseLLM*. This indicates that having more calibration samples can be beneficial in the pruning process. Perplexity decreases more rapidly from 8 samples to 32 samples. Beyond 32 samples, the rate at which perplexity decreases starts to slow down. In addition, increasing the number of calibration samples requires more computational resources, e.g., memory and computation time, in the overall pruning process. This suggests that the calibration sample sizes should be between 32 and 64 to ensure good performance while maintaining computational efficiency. Lastly, the figures show that *SparseLLM* achieves better perplexity than *SparseGPT* does with 32 or larger sample sizes for both OPT and LLaMA-2 models.

A.4 Computation Time vs. Model Sizes

We study how the computation time of *SparseGPT* and *SparseLLM* varies with different model sizes, as illustrated in Table 3 and Table 4 for OPT models and LLaMA-2 models. The rate at which the time taken increases is comparable for *SparseGPT* and *SparseLLM* as the model size increases. Additionally, computation time for *SparseLLM* are reported for a configuration of 4 to 10 epochs. As we have reported in Section 5, *SparseLLM* can reduce the training loss in as few as 2 to 3 epochs. This suggests that the proposed *SparseLLM* remains computationally efficient.

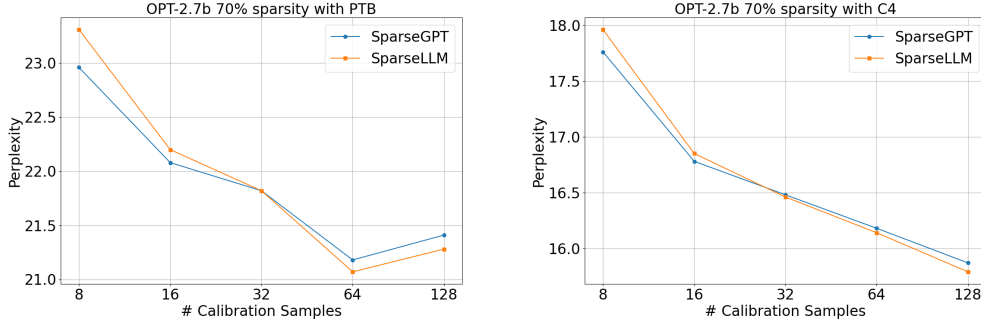


Figure 5: Sensitivity of OPT-2.7b on the calibration sample sizes for datasets PTB and C4.

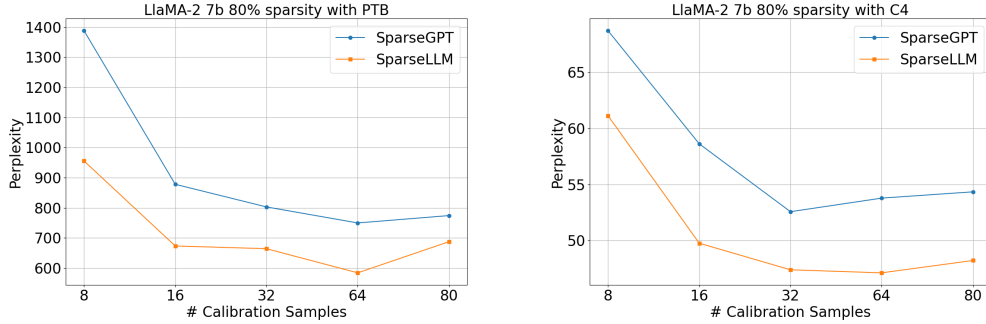


Figure 6: Sensitivity of LLaMA-2 7b models on the calibration sample sizes for datasets PTB and C4.

Table 3: Computation time in seconds of OPT models.

Method	OPT-125m	OPT-1.3b	OPT-2.7b	OPT-6.7b	OPT-13b	OPT-30b	OPT-66b
SparseGPT	1.47	4.03	4.36	8.15	10.46	20.94	34.78
SparseLLM	19.58	74.76	97.44	184.96	209.26	164.34	270.38

Table 4: Computation time in seconds of LLaMA-2 models.

Method	Llama-2 7b	Llama-2 13b
SparseGPT	179.08	314.95
SparseLLM	2201.99	4797.07

A.5 Experiment Results for Additional Models

Detailed results on perplexity and zero-shot task accuracy for additional models are reported in Table 5 and Table 6. Similar to other models, we report the perplexity results for the dense model next to the name of the model in the table. In particular, we see that SparseGPT and *SparseLLM* outperform Magnitude and Wanda with a significant margin across different sparsity. *SparseLLM* shares similar perplexity with SparseGPT for smaller sparsity but demonstrates much better perplexity for larger sparsity. Similar perplexity trends are observed across all three datasets, although, PTB, having the highest perplexity for each sparsity and method, is likely the most challenging dataset among the three. For the zero-shot task accuracy, we see that *SparseLLM* achieves comparable results to SparseGPT for smaller perplexity and the performance improvements are more obvious and significant with higher sparsity.

Table 5: Perplexity in high sparsity regimes ($\geq 70\%$); the lower the perplexity, the better.

OPT-125m (WikiText2 (WT2): 27.66; PTB: 38.99; C4: 26.56)												
Sparsity	70%			80%			90%			3:4		
Dataset	WT2	PTB	C4	WT2	PTB	C4	WT2	PTB	C4	WT2	PTB	C4
Magnitude	3806.96	3429.35	2263.37	4890.96	4121.49	3213.85	6613.18	5380.80	4475.29	-	-	-
Wanda	351.83	412.52	248.94	1912.45	2512.93	1066.86	4940.89	4337.27	3126.02	-	-	-
SparseGPT	239.26	265.83	156.33	2072.12	1952.85	1050.83	6131.57	6963.27	2443.33	1482.61	2215.44	657.26
SparseLLM	208.46	255.75	137.72	1358.10	1418.09	654.54	5291.64	5067.41	2003.09	914.87	1210.84	450.01
OPT-6.7b (WikiText2 (WT2): 10.86; PTB: 15.77; C4: 12.71)												
Sparsity	70%			80%			90%			3:4		
Dataset	WT2	PTB	C4	WT2	PTB	C4	WT2	PTB	C4	WT2	PTB	C4
Magnitude	7054.21	5437.44	4850.25	7937.49	5971.86	6031.54	2.4e4	2.5e4	2.1e4	-	-	-
Wanda	54.95	129.73	116.67	1493.58	1196.93	996.00	2.1e4	2.0e4	1.8e4	-	-	-
SparseGPT	12.27	18.90	15.28	31.04	51.26	29.42	8871.24	5713.57	3797.20	570.08	361.81	328.18
SparseLLM	12.16	18.39	14.93	23.96	39.32	26.97	2095.85	1842.48	953.44	83.36	128.99	62.11
OPT-13b (WikiText2 (WT2): 10.13; PTB: 14.52; C4: 12.06)												
Sparsity	70%			80%			85%			3:4		
Dataset	WT2	PTB	C4	WT2	PTB	C4	WT2	PTB	C4	WT2	PTB	C4
Magnitude	9037.12	7734.58	5909.47	1.1e4	9140.88	6340.22	1.3e4	1.3e4	9087.50	-	-	-
Wanda	30.94	39.26	33.31	4216.04	2894.77	2450.57	1.1e4	1.1e4	7244.96	-	-	-
SparseGPT	10.89	16.35	13.39	21.42	33.62	21.01	8408.03	6380.30	3416.23	4715.16	7454.37	2.11e4
SparseLLM	10.96	16.57	13.38	19.07	28.77	19.29	2052.27	1536.51	538.61	289.17	687.48	677.13

Table 6: Accuracy (%) of zero-shot tasks; the higher the accuracy, the better.

OPT-6.7b									
Sparsity	Method	BoolQ	RTE	HellaSwag	WinoGrande	ARC-e	ARC-c	OBQA	Mean
Dense		66.12	56.03	50.49	65.27	65.72	30.63	27.60	51.69
70%	SparseGPT	61.74	54.87	48.46	63.85	64.31	29.27	25.40	49.70
	SparseLLM	60.61	54.51	48.8	62.9	64.14	30.03	26.60	49.66
80%	SparseGPT	55.08	48.38	42.22	59.43	57.79	25.85	21.40	44.31
	SparseLLM	58.69	51.26	43.78	59.67	58.38	26.88	22.00	45.81
90%	SparseGPT	38.53	53.07	26.00	48.07	26.81	21.67	14.40	32.65
	SparseLLM	46.48	52.71	26.21	51.70	27.44	19.71	13.40	33.95
3:4	SparseGPT	46.70	54.15	28.82	51.07	32.45	18.17	15.40	35.25
	SparseLLM	53.49	53.42	36.24	53.51	43.94	22.61	17.40	40.09
OPT-13b									
Sparsity	Method	BoolQ	RTE	HellaSwag	WinoGrande	ARC-e	ARC-c	OBQA	Mean
Dense		65.87	57.76	52.44	66.02	67.82	33.46	28.62	53.14
70%	SparseGPT	63.03	54.87	50.89	65.43	67.47	32.85	26.40	51.56
	SparseLLM	63.85	55.23	50.73	65.67	66.46	31.83	27.20	51.57
80%	SparseGPT	59.72	52.35	46.82	61.48	62.50	31.23	21.80	47.99
	SparseLLM	60.89	53.07	46.19	62.12	62.21	30.38	23.00	48.27
90%	SparseGPT	47.49	52.71	33.17	51.54	39.98	21.33	17.80	37.72
	SparseLLM	53.43	52.71	38.19	52.96	46.68	25.26	17.40	40.95
3:4	SparseGPT	47.55	53.43	31.30	50.20	37.63	22.53	17.60	37.18
	SparseLLM	51.13	52.35	38.51	55.96	49.24	24.83	21.40	41.92